
Cross-layering between physical layer, medium access control, and routing in wireless ad-hoc networks

Jean-Michel Dricot*

OPERA Department – Wireless Communications Group,
Université Libre de Bruxelles,
1050 Bruxelles, Belgium
E-mail: jdricot@ulb.ac.be
*Corresponding author

Gianluigi Ferrari

Department of Information Engineering,
University of Parma,
Wireless Ad-hoc and Sensor Networks (WASN) Lab,
43124 Parma, Italy
E-mail: gianluigi.ferrari@unipr.it

Philippe De Doncker

OPERA Department – Wireless Communications Group,
Université Libre de Bruxelles,
1050 Bruxelles, Belgium
E-mail: pdedonck@ulb.ac.be

Abstract: Routing is a key issue in wireless ad-hoc networks. The goal of an efficient routing strategy is to set up routes so that the overall quality of communications will be the best possible. While the Open Systems Interconnection (OSI) reference model advocates for a clear separation of routing, access, and physical layers, in this paper we show that in scenarios with *strongly faded* communications, cross-layer interactions have to be carefully considered. More precisely, we compare the performance of the Ad-hoc On-demand Distance Vector (AODV) routing algorithm with that of one of its physical layer-oriented variants, denoted as AODV φ . It will be clearly shown that no single routing strategy is always optimal and that an intelligent information fusion at the Medium Access Control (MAC) level can be very beneficial.

Keywords: wireless networks; cross-layer; channel modelling; performance evaluation; fading.

Reference to this paper should be made as follows: Dricot, J.-M., Ferrari, G. and De Doncker, P. (2012) 'Cross-layering between physical layer, medium access control, and routing in wireless ad-hoc networks', *Int. J. Ad Hoc and Ubiquitous Computing*, Vol. 9, No. 3, pp.159–170.

Biographical notes: Jean-Michel Dricot is Associate Professor at the OPERA department – Wireless Communications Group. He received a MSc EEng and PhD from the Université Libre de Bruxelles. Then, he worked for France Telecom R&D (Orange Labs) before returning to academia in the ULB Machine Learning Group. His main research topics include cross layer optimisation, cognitive networks, and performance analysis. He acts as a frequent reviewer for several journals and is the author of several book chapters and papers and is the co-organiser of an international workshop dedicated to performance evaluation in wireless sensor networks.

Gianluigi Ferrari received his PhD from the University of Parma, Italy, in 2002. He is currently an Associate Professor at the University Parma. He was a Visiting Researcher at USC, Los Angeles, CA, USA (2000–2001), CMU, Pittsburgh, PA, USA (2002–2004), KMITL, Bangkok, Thailand (2007), and ULB, Belgium (2010). Since 2006, he has been the Coordinator of the Wireless Ad-hoc and Sensor Networks (WASN) Lab in the Department of Information Engineering of the University of Parma. As of today, he has published more than 150 papers in leading international journals and

conference proceedings, and a few chapter books and books. He is on the Editorial Boards of a few international journals and acts as TPC member for many international conferences.

Philippe De Doncker is Associate Professor at the Wireless Communications Group of the OPERA department (Université Libre de Bruxelles, Engineering school). During the last five years, he initiated and/or participated in the launch of nine funded research projects and was awarded for more than 1 million euros of research material. He is currently supervisor or co-supervisor of eight PhD theses. He is regularly invited as an expert in wireless communications. He received his Msc Physics Engineering degree and PhD degree from the University of Brussels.

1 Introduction

A wireless ad-hoc network consists of a large number of autonomous mobile nodes connected to each other directly and without the need for pre-existing configuration parameters or centralised infrastructures (Boukerche, 2008; Ramanathan, 2005). From an architectural point of view, a Mobile Ad-hoc NETWORK (MANET) is formed as a *multi-hop* architecture due to the limited transmission range of wireless transceivers and node mobility. Therefore, routing plays an important role in the operation of such networks: each node has to act as both router and host.

While the Open Systems Interconnection (OSI) reference model advocates for a clear separation of the routing, access, and physical layers, this distinction is often never achieved in several future generation wireless network architectures (Choi et al., 2009). In fact, the physical layer is very variable and its characteristics strongly influence the performance of MANETs. Therefore, its interaction with the upper layers often leads to unexpected and undesirable effects. This paper analyses the existing cross-layer interactions between the physical layer, the Medium Access Control (MAC) layer, and the routing strategy.

The remainder of this manuscript is organised as follows. In Section 2, we summarise related works and highlight the main contributions of our paper. In Section 3, the log-normal fading link model is introduced. Then, for a slotted MAC scheme, the conditional success probability of a transmission for a node, given the transmitter-receiver and interferences-receiver distances, is derived. Section 4 presents a few preliminaries on the simulation set-up and the considered routing algorithms. In Section 5, the interaction between the physical layer and the routing protocol is investigated. In Section 6, the interaction between MAC and routing layers is discussed. Section 7 concludes the paper.

2 Related work and contributions of this work

The goal of a routing algorithm is to find the best route according to a proper cost function. For instance,

possible strategies include shortest-path routing (Tan et al., 2003), energy-aware routing (Dietrich and Dressler, 2009; Park and Lee, 2008; Mohanoor et al., 2009), and highest stability (or least-congested) routing (Meng and Wu, 2008). Meanwhile, these approaches typically do not take into account the cross-layer interactions suggested in Akyildiz and Wang (2008), Dricot et al. (2005) and Choi et al. (2009), which clearly highlight the impact that physical layer has on routing efficiency. In particular, the Bit Error Rate (BER) at the end of a multi-hop route may, under certain conditions, represent a good indicator of the physical layer status (Tonguz and Ferrari, 2006). In particular, in Ferrari et al. (2008) a modified version of the Ad-hoc On-demand Distance Vector (AODV) protocol, denoted as MAODV, has been proposed, incorporating a simple power control strategy, which does not exploit routing information. Also, it has been recently shown that the Expected Transmission (ETX) count of a path, defined as the expected total number of packet transmissions (including retransmissions) required to successfully deliver a packet along that path, is a good indicator of the routing quality (De Couto, 2004).

The impact of the interactions between the OSI layers has received a significant attention in the last years. The interaction between the physical and the application layers (and, more precisely, VoIP and video throughput) has been quantified in Tobagi et al. (2007). The impact of the interference on the throughput (Vyas and Tobagi, 2006) and the connectivity (Dousse et al., 2005) has also been highlighted.

The main contributions of this paper, with respect to the existing literature, can be summarised as follows.

- We derive the probability of successful link transmission in network scenarios with
 - i wireless communication links subject to slow fading and
 - ii regular topologies.
- We analyse the impact of the wireless channel conditions (fading and attenuation) on the performance of a few routing protocols, thus

discussing on the relevance of routing protocol selection according to the propagation conditions.

- Finally, we look for a possible integration of routing information and power control at the MAC level.

Our results show that there exists a strong interaction

- between the channel characteristics and the routing strategy and
- between routing and MAC protocols.

3 The log-normal fading link model

We assume a narrowband log-normal block fading channel (Catedra and Perez, 1999). This model is implemented in the NS-2 simulator and will be used in Section 4.3 for the analysis of the cross-layer interactions. According to the log-normal fading model, the instantaneous ratio of transmit-to-receive power $X = P_{r-ref}/P_{t-ref}$ (non dimensional), at a reference distance d_{ref} (dimension: [m]), is assumed to have the following log-normal distribution:

$$f_X(x) = \frac{1}{x\sqrt{2\pi\sigma^2}} \exp\left[-\frac{(\ln x - \mu)^2}{2\sigma^2}\right] U(x)$$

where μ is the average pathloss attenuation (in a logarithmic scale), which can be evaluated through analytical models or empirical measurements, and σ is the standard deviation of X (adimensional). Most empirical studies support a standard deviation $\sigma = 4 \div 16$ dB. Alternatively (and in the model implemented by the NS-2), the path loss can be treated separately from the slow fading by letting $\mu = 0$ dB and setting

$$P_r = P_t \left(\frac{d_t}{d_{ref}}\right)^{-n} X \quad (1)$$

where P_r is the received power (dimension: [W]) at distance d_t (dimension: [m]), P_t is the transmit power (dimension: [W]), and n is the pathloss exponent (adimensional). Under the assumption that $d_{ref} = 1$ m (as considered in NS-2), it follows that the received power can be expressed as follows:

$$P_r = \frac{X P_t}{d_t^{-n}}. \quad (2)$$

A transmission on the considered link is successful if and only if the signal-to-noise and interference ratio (SINR) at the receiver, is above a pre-defined threshold θ . This threshold value depends, among other factors, on the receiver characteristics, the modulation and coding scheme, etc. (Rappaport, 1996). The SINR can then be written as

$$\text{SINR} \triangleq \frac{P_r}{P_{env} + P_{int}} \quad (3)$$

where P_{env} is the background noise power and P_{int} is the total interference power at the receiver, given by the sum of the received powers from interfering transmitters. In sufficiently dense networks, the transmission is mainly limited by the interference, i.e., $P_{env} \ll P_{int}$.

In the following, we consider a *regular* network topology, in the sense that every receiver has the same number of nearest neighbours and the same distance to any of these nearest neighbours. In reality, the distances will more likely be non-homogeneous and distributed around an average value. The impact of the topology is out of the scope of this paper and can be analysed, for example, following the approach in Liu and Haenggi (2005). Also, we consider a simple slotted asynchronous random access scheme, such that, in each timeslot, every node transmits with a given probability (obviously proportional to the traffic load). Being the considered slotted access scheme simpler than other channelisation schemes (such as time/frequency division multiple access), it will allow to derive a lower bound on the performance of communication networks with more sophisticated MAC protocols under use.

We now characterise the considered log-normal fading link model by proving a few theoretical results.

Theorem 1: *In a wireless network with log-normal faded links, slotted asynchronous access as described above, and regular topology, the success probability of a transmission over a single link, given (i) a fixed transmitter-receiver distance d_t and (ii) j interfering nodes at distance d transmitting at a common power P_c , can be approximated as follows:*

$$\mathcal{P}_s^{(j)} \approx \frac{1}{2} - \frac{1}{2} \int_0^\infty \frac{\exp\left[-\frac{(\ln y - \mu_j)^2}{2\sigma_j^2}\right]}{y\sqrt{2\pi\sigma_j^2}} \text{erf}\left(\frac{\ln \xi y}{\sigma\sqrt{2}}\right) dy \quad (4)$$

where $\text{erf}(z) \triangleq \frac{2}{\sqrt{\pi}} \int_0^z e^{-t^2} dt$,

$$\xi \triangleq \theta \frac{P_c}{P_r} \left(\frac{d_t}{d}\right)^n, \quad (5)$$

P_r is the transmit power at the link source, θ is the SINR threshold, and

$$\sigma_j^2 = \ln\left(\frac{e^{\sigma^2} - 1}{j} + 1\right) \quad (6)$$

$$\mu_j = \ln j + \frac{\sigma^2 - \sigma_j^2}{2}. \quad (7)$$

Proof: From equation (2), the total interference in a scenario with j interfering neighbours is

$$P_{int} \triangleq \sum_{i=1}^j P_i = \sum_{i=1}^j P_c d^{-n} X_i$$

where $\{X_i\}_{i=1\dots j}$ are log-normally distributed and represent the independent fading processes associated with the links originating at the interfering nodes.

The probability of successful link transmission in the presence of j interferers is

$$\begin{aligned} \mathcal{P}_s^{(j)} &\triangleq \mathbb{P} \{ \text{SINR} > \theta \mid j \text{ interferers} \} \\ &= \mathbb{P} \left\{ \frac{P_r d_t^{-n} X}{\sum_{i=1}^j P_c d^{-n} X_i} > \theta \right\}. \end{aligned}$$

By introducing the new RV $Y^{(j)} \triangleq \sum_{i=1}^j X_i$, it follows:

$$\begin{aligned} \mathcal{P}_s^{(j)} &= 1 - \mathbb{P} \left\{ X \leq \xi Y^{(j)} \right\} \\ &= 1 - \iint_{x \leq \xi y} f_{XY^{(j)}}(x, y) dx dy \end{aligned} \quad (8)$$

where $f_{XY^{(j)}}(x, y)$ is the joint probability density function of X and $Y^{(j)}$. Since X and $Y^{(j)}$ are independent, i.e., $f_{XY^{(j)}}(x, y) = f_X(x)f_{Y^{(j)}}(y)$, it follows that

$$\mathcal{P}_s^{(j)} = 1 - \int_0^\infty \left(\int_0^{\xi y} f_{Y^{(j)}}(y) f_X(x) dx \right) dy. \quad (9)$$

In the case of the log-normal fading, $Y^{(j)}$ corresponds to the sum of log-normal random variables with the same parameters. Following the approach proposed in Fenton (1960) and Schwartz and Yeh (1982), $Y^{(j)}$ can be approximated as a log-normal random variable, i.e.,

$$f_{Y^{(j)}}(y) \approx \frac{1}{y\sigma_j\sqrt{2\pi}} \exp \left[-\frac{(\ln y - \mu_j)^2}{2\sigma_j^2} \right] U(x)$$

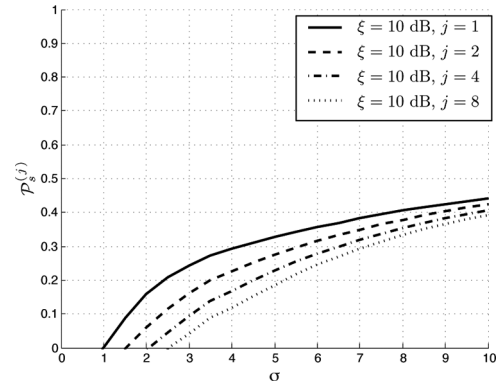
where σ_j^2 and μ_j are defined as in equations (6) and (7). Therefore, the probability of successful link transmission given by (9) becomes

$$\mathcal{P}_s^{(j)} = \frac{1}{2} - \frac{1}{2} \int_0^\infty \frac{\exp \left[-\frac{(\ln y - \mu_j)^2}{2\sigma_j^2} \right]}{y\sigma_j\sqrt{2\pi}} \operatorname{erf} \left(\frac{\ln \xi y}{\sigma\sqrt{2}} \right) dy.$$

□

A closed-form expression of $\mathcal{P}_s^{(j)}$ cannot be derived and its integral expression must be numerically evaluated. In Figure 1, $\mathcal{P}_s^{(j)}$ is shown, as a function of the log-normal fading power σ , for various values of the number of interferers j . In all cases, $\xi = 10$ dB – this corresponds to keeping the SINR threshold fixed. The obtained results suggest that a higher value of the standard deviation σ of the lognormal shadowing coefficient *improves* the connectivity properties of the network, as predicted by the results in Hekmat and Van Mieghem (2006); Miorandi et al. (2008). This is intuitively due to the fact that a higher value of the fading power σ^2 corresponds to a higher variability of its realisations (over a link). Therefore, on average long deep fades are reduced and, therefore, the success probability of a transmission over a single link increases. Should retransmissions be considered, this could be interpreted as the fact that in consecutive retransmissions there is a higher probability of finding the link unaffected by fading at least once.

Figure 1 Probability of link success $\mathcal{P}_s^{(j)}$ as a function of σ and for a fixed value of ξ . Various values of the number of active interferers j are considered



Corollary 1: *In a regular multi-hop network where a receiving node at the end of a link is subject to interferences from j active nodes, a sufficient condition to increase the link probability of success, given that the transmit power cannot be varied, is to select the closest possible neighbour as the next hop of the route.*

Proof: The probability of success on a single link subject to j interferers is given by expression (4) in Theorem 1. In this expression, the values $\mu_j \geq 0$, $\sigma_j \geq 0$ are strictly dependent on the characteristics of the fading process and cannot be modified. A simple analysis of the expression of $\mathcal{P}_s^{(j)}$ shows that this quantity can be maximised if ξ is minimised. Recalling the definition of ξ given in (5), one can easily conclude that the parameters θ , P_c , and d cannot be adjusted by the transmitters. Therefore, the two remaining available options for the transmitting node to minimise ξ are

- i increasing its transmit power P_t (this would have a negative impact on network performance) or
- ii to minimise the transmission distance d_t , i.e., to choose the closest possible node as the next hop for the route.

Since we are assuming that the transmit power cannot be varied, the second option is the only possible. □

Note that this coincides with the approach proposed in Ferrari et al. (2008) in the case of AWGN channels and strong line-of-sight scenarios. Unlike the AWGN case, in the considered shadowed fading scenario the distance to a neighbouring node can be obtained by means of well-known cooperative localisation techniques, such as those described in Dricot et al. (2009). On the other hand, another approach to estimate the distance is based on the transmission of multiple consecutive (short) detection packets. This second method is detailed in Appendix.

The following theorem provides a simple expression for the average (with respect to the number of interferers) probability of successful link transmission. This expression is derived by modelling the proposed

slotted MAC protocol under the assumption of a simple Bernoulli transmission model, which is supported by the analyses presented in Tobagi (1980) and Bertsekas and Gallager (1992, p.278).

Theorem 2: *In a log-normal faded network with slotted transmissions, where nodes transmit with probability q , the success probability of a transmission, given (i) a fixed transmitter-receiver distance d_t and (ii) N “dominant neighbours” at distance d transmitting at a common power P_c , is*

$$\mathcal{P}_s = \sum_{j=0}^N \binom{N}{j} \mathcal{P}_s^{(j)} q^j (1-q)^{N-j}.$$

Proof: The *dominant neighbours* are the nodes in the direct vicinity of the transmitter of interest. Indeed, since the received power decreases exponentially with the distance, one can assume that the total interference power is mainly due to the direct (i.e., one-hop) neighbour nodes only and, therefore, the total interference in a scenario with N possible interfering neighbours is

$$P_{\text{int}} \triangleq \sum_{i=1}^N P_i \Lambda_i$$

where $\{\Lambda_i\}_{i=1\dots N}$ is a sequence of stochastically independent Bernoulli distributed random variables with $\mathbb{P}\{\Lambda_i = 1\} = q$ and $\mathbb{P}\{\Lambda_i = 0\} = 1 - q$. The probability that j nodes among the N nodes interfere at the same moment is thus a binomial RV with parameters q and N :

$$\mathbb{P}\{j \text{ interferers} | q, N\} = \binom{N}{j} q^j (1-q)^{N-j} \quad (10)$$

and the total probability of link success in the presence of N possible interferers then becomes

$$\begin{aligned} \mathcal{P}_s &\triangleq \mathbb{P}\{\text{SINR} > \theta\} \\ &= \sum_{j=0}^N \underbrace{\mathbb{P}\{\text{SINR} > \theta | j \text{ interferers}\}}_{\mathcal{P}_s^{(j)}} \cdot \underbrace{\mathbb{P}\{j \text{ interferers}\}}_{\binom{N}{j} q^j (1-q)^{N-j}} \\ &= \sum_{j=0}^N \binom{N}{j} \mathcal{P}_s^{(j)} q^j (1-q)^{N-j}. \end{aligned}$$

□

In Figure 2, the link probability of success is presented as a function of the amount of active interfering nodes N and the probability of transmission q . In Figure 3, the link probability of success \mathcal{P}_s is presented as a function of σ and for various values of the probability of transmission q . In both figures, ξ is set to 10 dB. It can be observed from Figure 2 that, even if the amount of interferers increases, there remains a minimum achievable value for the link probability of success. This

lower bound is $\mathcal{P}_s^{\text{min}} = 0.185$. It is interesting to note that this is unlike in the fast fading (i.e., Rayleigh fading) scenario where the link probability of success rapidly decreases to $\mathcal{P}_s = 0$ as q increases (Liu and Haenggi, 2005).

Figure 2 Link probability success on a single link as a function of the probability of transmission q and the amount of neighbours N . The value of $\xi = 10$ dB and $\sigma = 10$ dB

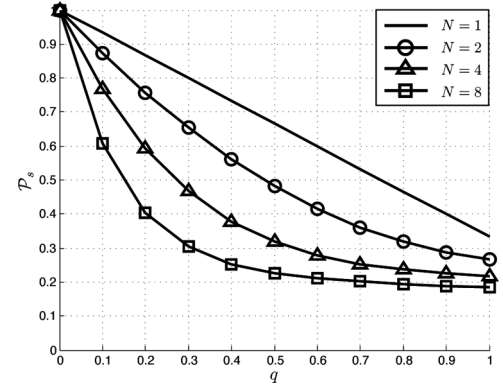
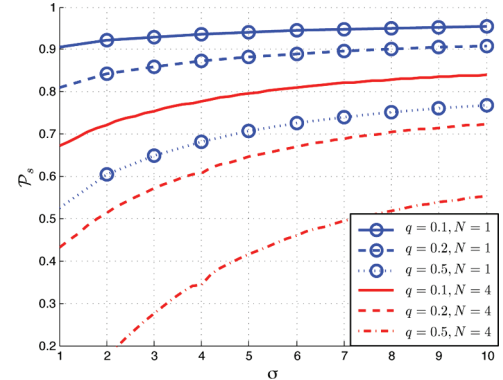


Figure 3 Link probability success on a single link in the case of the shadowing model and as a function of σ and the probability of transmission q . The value of $\xi = 10$ dB (see online version for colours)



4 Preliminaries on the simulation-based analysis

Sections 5 and 6 will present the key results of a simulation-based analysis of the cross-layer interactions between

- i the physical layer and the routing and
- ii the routing protocol and the MAC, respectively.

In order to perform this analysis, we first provide the reader with a few useful preliminaries on the Ad-hoc On-demand Distance Vector (AODV) routing algorithm and on one of its possible physical layer-oriented variants, denoted as AODV $_{\varphi}$. We conclude by summarising the main parameters of the considered NS-2 simulator and the relevant performance metrics.

4.1 The Ad-hoc On-demand Distance Vector routing protocol

The AODV routing protocol belongs to the class of *on-demand* routing strategies (Perkins, 2001; Belding-Royer, 2004): a route is created at the time a source needs to reach a destination. In order to locate the destination node, the source broadcasts a Route Request (RREQ) message all over the network. Each time an intermediate node is solicited, it adds an entry in its routing tables and builds a reverse path to the source. This flooding operation stops when the messages reach the destination or when a node has already the destination in its routing table. A unicast Route Reply (RREP) message is sent along the reverse path leading to the source. At that moment, the route is formed and kept in cache. When a link breaks, due to mobility or bad propagation conditions, a new route discovery is triggered (Perkins and Royer, 1999). Finally, for each destination the route lengths are regularly computed and only the shortest route is kept, i.e., the one with smallest hop count.

4.2 AODV φ : A physical layer-enhanced variant of the AODV protocol

The AODV φ routing algorithm is a variant of the AODV routing protocol. It implements the relaying strategy proposed in Corollary 1, i.e., it selects the closest possible neighbour as the next hop, when finding possible routes to the destination. More specifically, the following steps are taken in the route discovery phase.

- The source sends a RREQ message to its neighbours.
- Each node receiving the RREQ message builds the list of its neighbours and picks the closest one, to which the RREQ message is forwarded.
- The previous step is repeated for consecutive nodes, until the final destination is reached.
- The destination node replies with a unicast RREP message, as with the classical approach implemented in the AODV protocol.

Note that sequence numbers are used to avoid any loop creation and to optimise the route length, i.e., if a new route with less hops is detected, it is selected as the new route. Finally, as will be described in more detail in Section 6, the AODV φ protocol uses a power control strategy, at the MAC layer, to optimise multi-hop communications.

4.3 NS-2 parameters and performance metrics

The following three metrics are chosen in order to evaluate the performance of the routing protocols of interest.

- *The route throughput* (also referred to as packet delivery fraction): This metric is defined as the ratio between
 - i the data packets that successfully reach their destinations and
 - ii the total number of generated data packets.
- *The normalised routing load*: This metric is given by the ratio between the number of control packets transmitted during the simulation and the number of correctly delivered data packets. Intuitively, this metric quantifies the efficiency of a routing protocol in terms of control overhead needed to create and maintain communication routes. Obviously, it should be kept as low as possible.
- *The end-to-end delay*: is the average amount of time required for a packet to reach the destination on the route.

The other reference values for the simulation parameters are presented in Table 1.

Table 1 Reference values for the parameters used in the simulations

Number of nodes in the network	50
Area A [m \times m]	1500 \times 300
Node spatial density ρ_S [m $^{-2}$]	1.1×10^{-4}
MAC Protocol	IEEE 802.11 DCF
Attenuation model	Shadowing
Transmission bit rate R_b [Mb/s]	2
Carrier frequency f_c [MHz]	914
Max. transmit power P_t^{\max} [W]	0.282
Initial node energy [J]	30
Send buffer [pck]	64
Interface queue [pck]	64
Source type	Constant bit Rate (CBR)
Probability of transmission q	0.1
Minimum received power threshold P_{thresh} [W]	3.652×10^{-10} W
SINR Threshold θ [dB]	10
Simulation time [s]	6000
Mobility model	Random waypoint
Pause time [s]	600
Node speed v [m/s]	1

5 Interaction between routing and physical layer

5.1 Route throughput

Figures 4 and 5 show the route throughput for the AODV and the AODV φ routing protocols, respectively, as a function of the fading standard deviation σ and the pathloss exponent n . As can be observed from the results in these figures, for a given value of n , the

end-to-end route throughput is almost insensitive to the power of the fading. Referring back to Figure 3, it was shown that the *link* probability of success increases as the spread of the fading σ increases. However, in the ‘average’ networking scenario we simulated, each node has multiple neighbours (i.e., $N > 2$) and the probability of transmission is reasonable ($q = 0.1$). From Figure 3, it can be observed that the link probability of success for $q = 0.1$ and $N > 2$ is less sensitive on the value taken by σ .

Figure 4 Route throughput with the AODV routing protocol, as a function of the pathloss exponent n and fading standard deviation σ (see online version for colours)

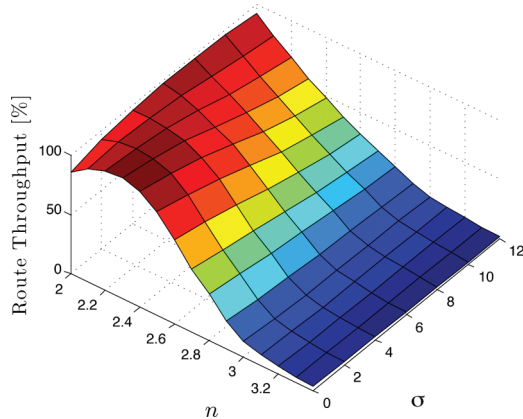
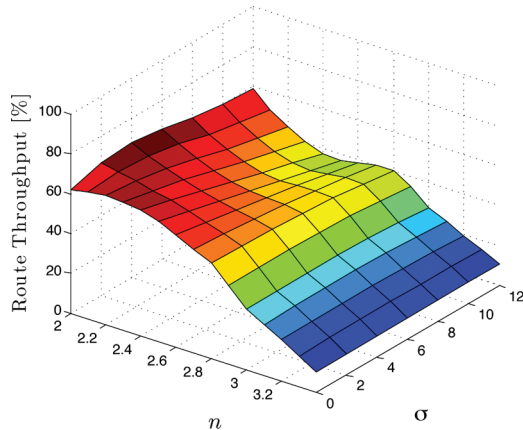


Figure 5 Routing throughput with the AODV φ routing protocol, as a function of the pathloss exponent n and fading standard deviation σ (see online version for colours)

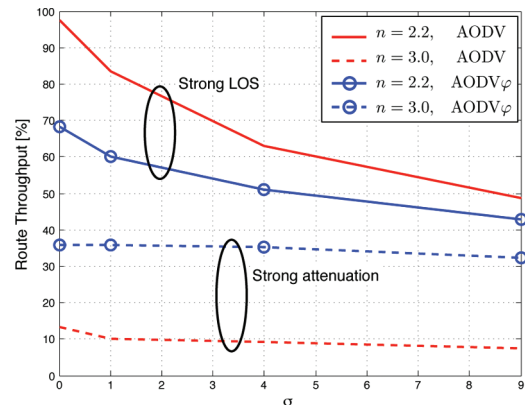


It is interesting to note that the *route* probability of success $\mathcal{P}_{s,route}$ depends on a successful transmission at *each* link and is, therefore, an exponential function of the average number of hops n_{hops} , that is $\mathcal{P}_{s,route} \propto (\mathcal{P}_s)^{n_{hops}}$. This explains why the AODV φ routing protocol (that selects, by construction, routes with a larger number of hops with respect to the AODV protocol) has a lower throughput when n is small. Finally, it can be observed that the pathloss exponent n has a different impact, depending on the used routing

protocol, on the route throughput. This suggests the existence of cross-layering.

In order to better understand the cross-layer interaction between physical layer and routing, we consider proper ‘slices’ of the three-dimensional performance surfaces shown in Figures 4 and 5. In particular, in Figure 6 the throughput is shown as a function of the fading intensity, for two possible values of n and considering both AODV and AODV φ protocols. It can be observed that, when the fading power increases, the performance of the AODV protocol, in terms of throughput, decreases significantly. This is an undesirable side effect of the longest hops strategy, i.e., when the hops are set to the maximum transmission distance, the received power is the lowest possible. Therefore, in the presence of strong fading, it is more likely that the SINR on the link will fall under the minimum threshold value and an outage will occur. On the other hand, by combining the expressions (2) and (3), one can see that since the AODV φ protocol selects routes with hops shorter than those selected by the AODV protocol, the corresponding SINR will be significantly higher and an outage event will occur less likely. From the results in Figure 6, it can also be observed that, when the pathloss exponent is high, the fading power plays little or no role.

Figure 6 Route throughput as a function of the fading standard deviation σ , considering two values of the pathloss exponent n (2.2 and 3). The AODV φ and AODV protocols are directly compared (see online version for colours)



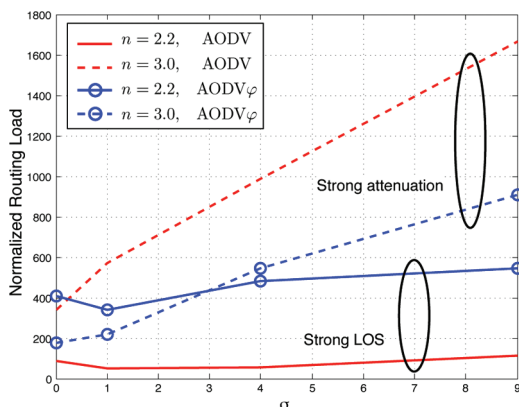
It is interesting to note that an alternative analysis of the impact of the fading is carried out, in the presence of a small-scale block fading (or Rayleigh fading), in Liu and Haenggi (2005). The authors find that the expression of the probability of link success depends only on

- i the pathloss exponent
- ii the transmit power
- iii the network topology.

5.2 Routing overhead

In Figure 7, the normalised routing load is shown as a function of the fading standard deviation σ , considering two values for n (namely, 2.2 and 3). It can be seen that, in the case of a limited attenuation (strong line-of-sight), the load incurred by the AODV $_{\varphi}$ protocol is high since the routes contain a large number of relaying nodes and this requires a substantial amount of control messages to create and maintain them. When the attenuation increases, the normalised routing load with the AODV protocol increases significantly and exceeds that of the AODV $_{\varphi}$ protocol. This is due to the larger number of route repairs triggered by the ‘fragile’ long hops selected by the AODV protocol and the increasing length of the routes. Note that a characteristic feature of the AODV $_{\varphi}$ protocol is that the normalised routing load seems to be almost insensitive on the attenuation, i.e., on the value of n .

Figure 7 Normalised routing load as a function of the fading standard deviation σ , considering two values of the pathloss exponent n (2.2 and 3). The AODV $_{\varphi}$ and AODV protocols are directly compared (see online version for colours)



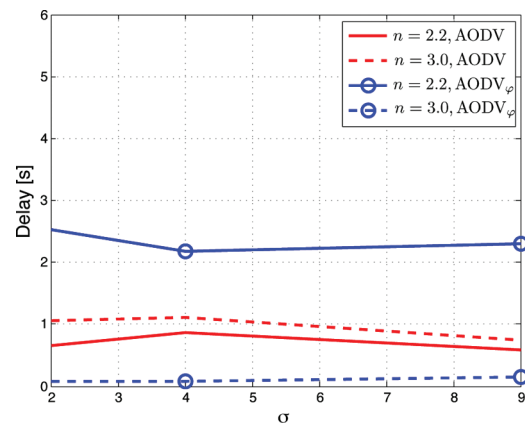
We also remark that node mobility has a clear impact on the performance of the considered routing protocols. Indeed, when the attenuation is high, the probability that a receiving nodes leaves the coverage zone of the transmitter is high, and this explains the poor performance of the AODV protocol in presence of strong attenuation. On the other hand, as will be described in detail in Subsection 6.1, in the initial phase of the AODV $_{\varphi}$ protocol, once the nearest neighbour is selected for the next hop, the transmit power of the link source is selected in order to prevent multiple access collisions. As will be clear in the following, this guarantees that the receiver tends to remain longer in the coverage zone. Therefore, the rate at which route reconstruction is triggered tends to remain low.

5.3 End-to-end delay

In Figure 8, the end-to-end delay is shown as a function of the fading standard deviation σ , considering

various values of the pathloss exponent n (i.e., various attenuation scenarios). It can be observed that, in the AODV case, the delay is approximately the same in the presence of either strong ($n=3$) or light ($n=2.2$) attenuation. In the AODV $_{\varphi}$ case, instead, the delay is high only in the presence of light attenuation, as the AODV $_{\varphi}$ protocol selects routes with larger numbers of hops than those selected by the AODV protocol. On the opposite, in the presence of strong attenuation, the AODV $_{\varphi}$ protocol outperforms the AODV protocol since the routes are more stable and the link probability of outage (and, therefore, the time spent for retransmissions) is significantly lower.

Figure 8 End-to-end delay as a function of the fading standard deviation σ , considering two values of the pathloss exponent n (2.2 and 3). The AODV $_{\varphi}$ and AODV protocols are directly compared (see online version for colours)



5.4 Discussion

It has been shown that the use of a routing protocol derived from physical layer considerations (i.e., the AODV $_{\varphi}$ routing protocol) can significantly improve the route throughput and reduce the normalised routing load in a scenario with strong attenuation. On the opposite, classical approaches (i.e., the AODV protocol) give better results when the attenuation is limited. Recent work has shown that the attenuation level (i.e., the pathloss exponent n) can be accurately estimated by a node (Srinivasa and Haenggi, 2007). Therefore, the routing strategy should be selected according to the detected level of attenuation.

6 Interaction between the routing and the medium access control

6.1 Impact of power control

The routing algorithm derived from Corollary 1 builds a route by using the shortest possible hops. Unlike the approach proposed in Yan et al. (2009) and Ramanathan and Rosales-Hain (2000), where a common (‘optimal’)

power control is assigned to each node, we evaluate the impact of a simple, yet effective, local assignment strategy. In other words, the transmit power is adjusted on a single-hop basis. Even if this strategy is intuitively simple, in most scenarios the link length may vary and this may lead to an increase of the collisions at the MAC level. Therefore, in this scenario the hidden terminal problem must be suitably reconsidered, taking into account non-homogeneous transmit powers set on the basis of an effective power control strategy.

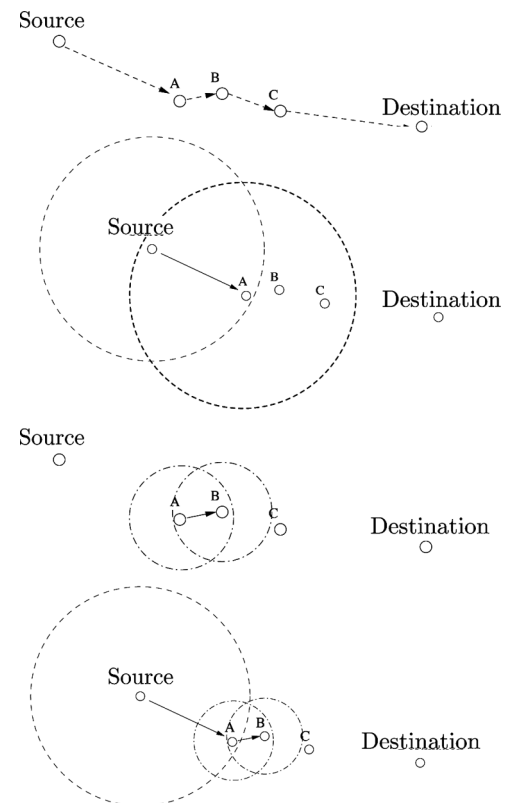
For the purpose of illustration, let us consider the 4-hop route (more generally, this could be a portion of a longer route) shown in Figure 9(a). At a generic time, a transmission occurs between the Source and node A: this is shown in Figure 9(b). As the nodes use an RTS/CTS mechanism (according to the IEEE 802.11 DCF protocol), the region locked around the Source and node A is quite large and the other nodes (i.e., nodes B and C) cannot interfere with the communication. Once the Source node has completed its transmission to node A, the latter node needs to forward the received data to node B and initiates an RTS/CTS exchange with power control. Nodes A and B are close to each other: the region locked is smaller than that previously locked and does not include the Source. This is shown in Figure 9(c). The notion that the communication between nodes A and B is taking place, however, is unknown to the source, which might decide to send another packet to node A. The Source then sends a RTS request, as shown in Figure 9(d), resulting in a collision in the transmission from node A to node B.

Furthermore, as shown in Theorem 2 and observed in Figure 3, we remark that a collision in the presence of a simple power control strategy will likely occur if

- i the traffic load is high (i.e., the probability of transmission q is high) and/or
- ii the number of dominant neighbours N is high (i.e., in dense networks).

Owing to attenuation and shadowing, it is accurate to assume that most of the RTS/CTS signaling perceived by a node will take place in its neighbourhood. Since a node has a routing table with information related to its neighbours, it is possible to use this routing information to perform a power control at the MAC layer. In other words, a routing/MAC cross-layer power control strategy is considered. The key idea of this power control strategy is that of considering the farthest neighbouring node and, then, set the transmit power in order to make this node perceive the RTS message (even if this node is *not* the next node along the route for which the current node is acting as a relay). This guarantees that all neighbouring nodes (possibly acting and sources or relays of nearby routes) will not start simultaneous transmissions, thus interfering with the considered node. This strategy is described by Algorithm 1.

Figure 9 Possible collision situations in an IEEE 802.11 network with MAC-level power control. The four subfigures represent the time evolution of the transmission scenario in the considered 4-hop route



Algorithm 1 Link-level cross-layer power control

Require: A transmitting node \mathcal{N}_i , its neighbor table \mathcal{T} extracted from the local routing table \mathcal{R} at node \mathcal{N}_i , the next-hop node \mathcal{N}_{i+1} on the route.

Ensure: Minimum transmit power P_{t-i} ([dBm]) at the i -th node to reach the $(i+1)$ -th node avoiding collisions in the common medium.

```

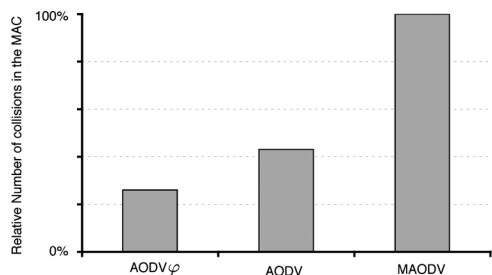
 $P_{\text{thresh}} \leftarrow$  minimum receive power
 $\theta \leftarrow$  required SINR
 $n \leftarrow$  pathloss exponent
 $d \leftarrow \text{dist}(\mathcal{N}_i, \mathcal{N}_{i+1})$ 
 $\text{size} \leftarrow$  number of elements in  $\mathcal{T}$ 
for  $\text{current} = 1$  to  $\text{size}$  do
     $\mathcal{N}_{\text{current}} \leftarrow$  next element in  $\mathcal{T}$ 
    if  $\text{dist}(\mathcal{N}_i, \mathcal{N}_{\text{current}}) > d$  then
         $d \leftarrow \text{dist}(\mathcal{N}_i, \mathcal{N}_{\text{current}})$ 
    end if
end for
 $P_{t-i} [\text{dBm}] \leftarrow P_{\text{thresh}} [\text{dBm}] + 10n \log(d) \theta [\text{dB}] + \theta [\text{dB}]$ 
    
```

In order to highlight the impact of the interaction between routing and MAC protocol, the number of collisions at the MAC level has been evaluated considering:

- i the AODV protocol (no power control)
- ii the MAODV protocol (Ferrari et al., 2008) (simple power control)
- iii the AODV φ protocol (cross-layer power control).

The corresponding results are shown in Figure 10. It can be observed that the fusion of the information contained in the routing tables significantly improves the probability of choosing the appropriate transmit power level.

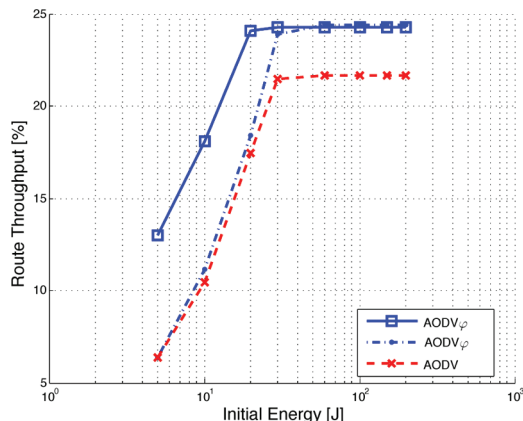
Figure 10 Comparison of the relative amount of collisions with the power control strategies used by the corresponding routing protocols. The pathloss exponent is $n = 3$ and the probability of transmission is $q = 0.1$



6.2 Impact of initial energy

In the presence of autonomous battery-powered devices (such as, for example, in mobile Wi-Fi systems), conserving energy is a key design goal (Jones et al., 2001). The power control algorithm used by the AODV φ protocol allows each node to reach the next node along the route, still guaranteeing no collisions with the dominant neighbours, with the lowest energy consumption and leads to slow energy depletion at the nodes. Consequently, a longer network lifetime is observed. For instance, in Figure 11 the route throughput is shown, as a function of the fixed

Figure 11 Route throughput, as a function of the initial energy, in a strongly faded scenario ($n = 3$), considering AODV, MADOV, and AODV φ protocols (see online version for colours)



initial energy found at each node, considering AODV, MAODV, and AODV φ protocols. The scenario is the one used throughout this paper and is described in Table 1. As one can see, for low values of the initial node energy, the AODV φ protocol almost *doubles* the route throughput of the AODV protocol. This relative performance improvement tends to reduce (to approximately 10%) for increasing values of the initial energy. As expected, the route throughput saturates beyond a critical value of the initial node energy. One can see that the saturation initial energy threshold for the AODV φ protocol (approximately 30 J) is lower than in the case with the AODV protocol (approximately 60 J).

7 Conclusions

In this paper, we have investigated the possible cross-layer interactions between physical layer, MAC protocol, and routing protocol in strongly faded scenarios. It has been shown that the routing strategy should be adapted according to the propagation conditions (*routing-physical layer interaction*). More precisely, a shortest-hop strategy is to be preferred when the attenuation level is sufficiently high and is not very sensitive to the fading intensity. It has also been shown that the routing strategy has a strong impact on the collision probability at MAC layer (*routing-MAC layer interaction*). In order to reduce the number of collisions, it has been proposed a simple, yet effective, local transmit power control strategy, based on the exploitation, at the MAC layer, of information from the routing layer. The obtained results show that the proposed cross-layer routing protocol design may lead, in strongly faded scenarios (with strong attenuation), to a significant performance gain.

Acknowledgement

This work was supported in part by the Belgian National Fund for Scientific Research (FRS-FNRS).

References

Akyildiz, I.F. and Wang, X. (2008) ‘Cross layer design in wireless mesh networks’, *IEEE Transactions on Vehicular Technology*, Vol. 57, No. 2, pp.1061–1076.

Belding-Royer, E.M. (2004) ‘Routing approaches in mobile ad hoc networks’, *Mobile Ad Hoc Networking*, Institute of Electrical and Electronics Engineers.

Bertsekas, D. and Gallager, R. (1992) *Data Networks*, 2nd ed., Prentice-Hall, Inc., Upper Saddle River, NJ, USA, p.278.

Boukerche, A. (Nov. 2008) ‘Algorithms and protocols for wireless’, *Mobile Ad Hoc Networks*, Wiley-IEEE Press.

Catedra, M.F. and Perez, J. (1999) *Cell Planning for Wireless Communications*, Artech House, Inc., Norwood, MA, USA.

- Choi, J., Park, K., and Kim, C-k. (2009) 'Analysis of cross-layer interaction in multirate 802.11 w lans', *IEEE Transactions on Mobile Computing*, Vol. 8, No. 5, pp.682–693.
- De Couto, D.S.J. (2004) *High-Throughput Routing for Multi-Hop Wireless Networks*, PhD Thesis, Massachusetts Institute of Technology, Department of Electrical Engineering and Computer Science, Boston, MA, USA.
- Dietrich, I. and Dressler, F. (2009) 'On the lifetime of wireless sensor networks', *ACM Trans. Sen. Netw.*, Vol. 5, No. 1, pp.1–39.
- Dousse, O., Baccelli, F. and Thiran, P. (2005) 'Impact of interferences on connectivity in ad hoc networks', *IEEE/ACM Trans. Netw.*, Vol. 13, No. 2, pp.425–436.
- Dricot, J-M., Bontempi, G. and De Doncker, P. (2009) *Sensor Networks: Where Theory Meets Practice*, chapter 'Static and Dynamic Localization Techniques', Springer.
- Dricot, J-M., De Doncker, P. and Zimányi, E. (2005) 'Multivariate analysis of the cross-layer interaction in wireless network simulations', *Proc. of the Int. Workshop on Wireless Ad-hoc Networks (IWVAN'05)*, London, UK.
- Fenton, L.F. (1960) 'The sum of log-normal probability distributions in scattered transmission systems', *IRE Trans. Commun. Systems*, Vol. 8, pp.57–67.
- Ferrari, G., Malvassori, S.A. and Tonguz, O.K. (2008) 'On physical layer-oriented routing with power control in ad-hoc wireless networks', *IET Communications*, Vol. 2, No. 2, pp.306–319.
- Hekmat, R. and Van Mieghem, P. (2006) 'Connectivity in wireless ad-hoc networks with a log-normal radio model', *Mob. Netw. Appl.*, Vol. 11, No. 3, pp.351–360.
- Jones, C.E., Sivalingam, K.M., Agrawal, P. and Chen, J.C. (2001) 'A survey of energy efficient network protocols for wireless networks', *Wirel. Netw.*, Vol. 7, No. 4, pp.343–358.
- Liu, X. and Haenggi, M. (2005) 'Throughput analysis of fading sensor networks with regular and random topologies', *EURASIP J. Wirel. Commun. Netw.*, Vol. 2005, No. 4, pp.554–564.
- Meng, L. and Wu, W. (2008) 'Dynamic source routing protocol based on link stability arithmetic', *Proceedings of the 2008 International Symposium on Information Science and Engineering (ISISE '08)*, Washington DC, USA, pp.730–733.
- Miorandi, D., Altman, E. and Alfano, G. (2008) 'The impact of channel randomness on coverage and connectivity of ad hoc and sensor networks', *IEEE Trans. Wireless Commun.*, Vol. 7, No. 3, pp.1062–1072.
- Mohanoor, A.B., Radhakrishnan, S. and Sarangan, V. (2009) 'Online energy aware routing in wireless networks', *Ad Hoc Netw.*, Vol. 7, No. 5, pp.918–931.
- Park, G. and Lee, S. (2008) 'A routing protocol for extend network lifetime through the residual battery and link stability in MANET', *Proceedings of the WSEAS International Conference on Applied Computing Conference (ACC'08)*, Istanbul, Turkey, pp.199–204.
- Perkins, C.E. (2001) *Ad hoc Networking*, Addison-Wesley, Upper Saddle River, NJ, USA.
- Perkins, C.E. and Royer, E.M. (1999) 'Ad-hoc on-demand distance vector routing', *Proc. of the Second IEEE Workshop on Mobile Computer Systems and Applications (WMCSA'99)*, New Orleans, Louisiana, USA, pp.90–100.
- Ramanathan, R. (2005) 'Challenges: a radically new architecture for next generation mobile ad hoc networks', *Proc. of the 11th Annual International Conference on Mobile Computing and Networking (MobiCom'05)*, Cologne, Germany, pp.132–139.
- Ramanathan, R. and Rosales-Hain, R. (2000) 'Topology control of multihop wireless networks using transmit power adjustment', *Proc. IEEE Conf. on Computer Commun. (INFOCOM)*, Tel Aviv, Israel, pp.404–413.
- Rappaport, T.S. (1996) *Wireless Communications: Principles and Practice*, IEEE Press, Piscataway, NJ, USA.
- Schwartz, S.C. and Yeh, Y.S. (1982) 'On the distribution function and moments of power sums with log-normal components', *Bell Systems Technical Journal*, Vol. 61, No. 7, pp.1441–1462.
- Srinivasa, S. and Haenggi, M. (2007) 'Modeling interference in finite uniformly random networks', *Proc. International Workshop on Information Theory for Sensor Networks (WITS '07)*, Santa Fe, NM, USA.
- Tan, K., Zhang, Q. and Zhu, W. (2003) 'Shortest path routing in partially connected ad hoc networks', *Proc. of the IEEE Global Telecommunications Conference (GLOBECOM'03)*, San Francisco, CA, USA, Vol. 2, pp.1038–1042.
- Tobagi, F. (1980) 'Analysis of a two-hop centralized packet radio network—Part I: slotted ALOHA', *IEEE Trans. Commun.*, Vol. 28, No. 2, pp.196–207.
- Tobagi, F.A., Vyas, A.K., Ha, S. and Awoniyi, O. (2007) 'Interactions between the physical layer and upper layers in wireless networks', *Ad Hoc Netw.*, Vol. 5, No. 8, pp.1208–1219.
- Tonguz, O.K. and Ferrari, G. (2006) *Ad Hoc Wireless Networks: A Communication-Theoretic Perspective*, John Wiley and Sons, Chichester, UK.
- Vyas, A. and Tobagi, F. (2006) 'Impact of interference on the throughput of a multihop path in a wireless network', *Proceedings of the IEEE third International Conference on Broadband Communications, Networks and Systems (BROADNETS)*, San Jose, CA, USA, pp.1–10.
- Yan, H., Li, J., Sun, G., Guizani, S. and Chen, H-H. (2009) 'A novel power control mac protocol for mobile ad hoc networks', *Int. J. Sen. Netw.*, Vol. 4, No. 4, pp.230–237.

Appendix

According to expression (2) for the received power, should the realisation of X be available, the distance from the transmitter could be inferred by the receiver from the received power as

$$d = \left(\frac{X P_t}{P_r} \right)^{\frac{1}{n}}.$$

However, X is not a priori known. Nevertheless, if successive packets are sent by a node (as part of a detection phase), the receiving node can compute its distance from the transmitter by limiting the negative

influence of fading. This is intuitively due to the time-varying nature of fading, and can be formalised as follows.

Assuming that m consecutive (and identical) detection packets are transmitted, the average received power at the receiver can be expressed as

$$\overline{P}_r^{(m)} = \frac{1}{m} \frac{\sum_i^m X_i P_t}{d_t^n} = \frac{1}{m} \underbrace{\sum_i^m X_i}_{\triangleq Y} \frac{P_t}{d_t^n} = \frac{Y P_t}{d_t^n}$$

where $\{X_i\}_{i=1}^m$ are the fading realisations over the consecutive transmissions. Since consecutive fading realisations are independent and equally distributed (as described in Section 3), one can conclude that

$$\begin{aligned} \mathbb{E}[Y] &= e^{\sigma^2/2} \\ \text{Var}[Y] &= \frac{\text{Var}[X]}{m} = \frac{\sigma^2}{m}. \end{aligned}$$

The ratio between standard deviation and average value of a random variable is a good indicator of the variability, around the average, of the random variable: the smaller this ratio, the more concentrated

the realisations of the random variable around its average value. Considering the ratio $\sqrt{\text{Var}[Y]}/\mathbb{E}[Y]$, representative of the fading variability around its average value, it then follows that

$$\begin{aligned} \lim_{m \rightarrow \infty} \frac{\sqrt{\text{Var}[Y]}}{\mathbb{E}[Y]} &= \lim_{m \rightarrow \infty} \frac{\sigma}{m\sqrt{m} e^{\sigma^2/2}} \\ &= \frac{\sigma}{e^{\sigma^2/2}} \lim_{m \rightarrow \infty} \frac{1}{m\sqrt{m}} = 0 \end{aligned}$$

where $\sigma/e^{\sigma^2/2}$ corresponds to the ratio $\sqrt{\text{Var}[X]}/\mathbb{E}[X]$ over a single transmission. It is immediate to conclude that by considering a sufficiently large number m of retransmissions, the variability of the fading can be significantly reduced. For instance, considering $m = 5$ consecutive retransmissions reduces the variability by a factor $1/(5\sqrt{5}) \simeq 0.09$, i.e., by more than 10 times.

Finally, we remark that the transmission time of a small number (e.g., $m = 5$) of short detection packets is negligible, with respect to the transmission duration of regular data packets. Therefore, the proposed strategy for estimating the distance from the transmitter has a negligible impact on the system performance.